Excellent Surface Enhanced Raman properties of Titanate nanotube-dopamine-Ag triad through efficient substrate design and LSPR matching

Graham Dawson,*[a] Xiaorong Cheng,[b] Anthony Centeno,[c] Yulia Pilyugina,[a] Wentian Niu[a] and Ruochen Liu[a]

graham.dawson@xjtlu.edu.cn

Declarations

Funding **(information that explains whether and by whom the research was supported)**

This work was supported by Suzhou Institute of Industrial Technology Research Fund (Grant No. SGYKJ201705 and 2017kyqd010), Xi'an Jiaotong Liverpool University Research Development Fund and Key Programme Special Fund in XJTLU (KSF-E-02).

Conflicts of interest/Competing interests (include appropriate disclosures) There are no conflicts to declare.

Availability of data and material (data transparency) Supporting information available.

Code availability (software application or custom code) Not applicable

Authors' contributions (optional: please review the submission guidelines from the journal whether statements are mandatory) Graham Dawson, Xiaorong Cheng and Anthony Centeno contributed to the conception and design of the study. FDTD calculations were performed by Anthony Centeno. Experiments were performed by Wentian Niu, Yulia Pilyugina and Ruochen Liu. Manuscript was written by Graham Dawson and Anthony Centeno and commented upon by all authors.

Relevance Summary

In this work a novel triad nanocomposites containing trititanate nanotubes, Ag nanoparticles and dopamine were prepared and the SERS properties were measured experimentally. Control over the size and position of the Ag nanoparticles in the TiNT-dop-Ag system, along with the Localised Surface Plasmon Resonance (LSPR) of the Ag particles matching the Raman excitation wavelength, gives a SERS enhancement greater than 6 orders of magnitude. Electromagnetic modelling was used to provide a theoretical basis for these results.

[a] *Department of Chemistry, Xi'an Jiaotong Liverpool University, Suzhou, Jiangsu, 215123, P. R. China.*
[b] *Suzhou Vocational Institute of Industrial Technology, Suzhou, Jiangsu, 215104, P. R. China.*
[c] *University of Glasgow, School of Engineering, Glasgow, United Kingdom G12 8QQ (previously at Department of Electrical and Electronic Engineering, Xi'an Jiaotong Liverpool University, Suzhou, Jiangsu, 215123, P. R. China.*

In this work a novel triad nanocomposite containing trititanate nanotubes, Ag nanoparticles and dopamine was prepared and the SERS properties measured experimentally. Control over the size and position of the Ag nanoparticles in the TiNT-dop-Ag system, along with the Localised Surface Plasmon Resonance (LSPR) of the Ag particles matching the Raman excitation wavelength, gives a SERS enhancement greater than 6 orders of magnitude. Electromagnetic modelling was used to provide a theoretical basis for these results.

1. Introduction

Surface enhanced Raman scattering (SERS) is a powerful analytical technique for chemical sensing of trace amounts of analyte, which provides in-depth structural information. To date published results on SERS have typically used silver (Ag) or gold (Au) nanoparticles, and the dominant enhancement mechanism is considered to be from the increased electric field due to the Localized Surface Plasmon Resonance (LSPR) of the metal nanoparticles. There is also chemical enhancement which for a system including a metal particle, or substrate, can result in a transfer of electrons between the highest occupied molecular orbital (HOMO) and the fermi level of the metal. [1-4]

The preparation of titanate nanotubes was first reported by Kasuga *et al*. [5] through the hydrothermal treatment of TiO_2 with 10 M NaOH. These nanotubes have a porous structure and high surface area. In addition, the composition of the nanotubes was subsequently identified as trititanate [6-10], $H_2Ti_3O_7$. There has, furthermore, been a recent resurgence in interest in titanate nanomaterials due to their emergence as an electrode material in sodium battery research. [11, 12] In this context, understanding the surface properties, and the improvement of these properties, is an important subject in the field.

There has been a great deal of research in the structure and applications of polydopamine, with many researchers proposing different polymer and aggregation structures, for example [13]. Our novel work on the TiNT-dopamine system showed that dopamine exists in the monomeric form on the nanotube surface; however, it exists in closer proximity than expected, causing the promotion of electron injection and charge separation to the system after modification. [14] Additionally, the modification resulted in a colour change and a shoulder in the measured UV-vis absorbtion spectrum, stemming from the created charge transfer complex.

There is a vast amount of research on materials based on TiO_2 in nanotube arrays reported with a high SERS enhancement and photocatalytic ability. They have, in addition, shown promise as substrates for sensitive and recyclable SERS detection. [15-18] These materials are, however, normally highly ordered and grown directly on a Ti foil substrate.

We have recently investigated semiconductor SERS for TiNT modified with catechol based organic modifiers and found that the HOMO level of the system was located on the organic modifier of the charge transfer complex. [19] In addition, the catechol compounds studied resulted in band gaps for the composite being close to the laser wavelength typically used for Raman spectroscopy. Inspired by these results, the existence of the dopamine monomers and amine tail group allows us to exploit the self-assembly on the TiNT surface by dopamine to form a triad with Ag nanoparticles. This was achieved through controlled assembly via a novel fabrication pathway, resulting in excellent control over the size and position of the Ag nanoparticles. This, along with the LSPR wavelength of the metal particle matching the Raman excitation wavelength, endows the composite with SERS enhancement greater than 6 orders of magnitude.

2. Experimental Section

2.1 Sample preparation

Preparation of TiNT via hydrothermal method. Firstly, NaOH (8 g) was dissolved in MilliQ water (20 mL) to prepare 10 M NaOH solution. Next, TiO_2 (1 g) was placed in Teflon liners with the NaOH. The liners were then put into autoclave stainless steel jackets and placed in the oven at 140 ^{o}C for 72 hours. The samples were subsequently transferred to a beaker with MilliQ water (20 mL) and left stirring. The sample was filtered and washed with 1 M HCl (50 mL) and MilliQ water until; a pH of 7 was obtained before the resultant titanium nanotubes (TiNT) were finally dried, ground and collected.

Modification of TiNT with dopamine. A portion of TiNT (0.3 g) was taken and dispersed in MilliQ water (20 mL) by sonication. The resultant dispersion was then mixed with dopamine hydrochloride (10 wt %) and left stirring for 72 hours at room temperature. At first, both white solutions changed their colour to orange after dopamine chloride was added; however, at the end of the

reaction they became light-brown. Resultant products were filtered and each sample was washed with 50 mL of MilliQ water and 20 mL of ethanol. Finally, the samples were dried in an oven, ground and collected.

Preparation of nanosystems with silver. An aqueous solution of 0.1 M NH_3 (~15 mL) was added dropwise to the solution of 0.1 M $AgNO_3$ (2 mL) until it became transparent. Then, in the first round-bottom flask, TiNT-dopamine (0.1091 g) was placed the prepared $[Ag(NH_3)_2]^+$ solution (5.5 mL) and MilliQ water (25 mL) was finally added to the flask. The sample was left stirring for 72 hours at room temperature. The resultant product was a grey-brown sample, which was then filtered and washed with 50 mL of MilliQ water and 20 mL of ethanol. Samples were ultimately dried in an oven, ground and collected.

2.2 Sample characterization

UV-Vis spectra were measured using an Agilent Technologies Cary 300 Series UV-Vis spectrophotometer. The morphology of the nanostructures was recorded using a transmission electron microscope (TEM, FEI Tecnai F20) operating at 200 kV. The Surface Enhanced Raman Spectroscopy (SERS, HORIBA Scientific XploRA, Laser: 532nm Filter: 10 %; Hole: 300; Slit: 100; Grating: 1200T; Microscope:X50LWD; RTD exposure time: 1s, Exposure time(s): 5, Accumulation Number: 5) was used to detect the enhancement of the Raman signal, produced by different concentrations of methylene blue dropped on the nanosystem thin film. The thin films were prepared by dispersing the nanosystems in MilliQ water or ethanol and drop casting it on the surface of the glass slides. This process was optimised as shown in Table S1.

2.3 Electromagnetic Modelling

Calculations of the optical and electrodynamic properties of the Ag nanostructures were undertaken using the Finite-difference time-domain (FDTD) method. For the FDTD calculations a 3-D total field scheme is used. Following convergence testing a grid resolution of 2 nm in each direction was used. In addition, the dielectric function of the Ag nanoparticles was modelled with a combined Drude–Lorentz model. [20] To prevent non-physical reflections from the extremities of the FDTD workspace Perfectly Matched Layers (PML) were placed at the boundaries. All FDTD calculations were carried out using the open source MEEP FDTD code run on a blade node of the Tianhe-2 Guangzhou supercomputer (2x12 core, Xeon E5-2692V2, 64GB memory). Finally, the simulations were run for enough time steps to ensure convergence. Electric field plots were obtained using Matlab scripts [21] which took the output of the FDTD simulations for points around the Ag nanoparticle and TiNT. A diagram showing the polarization and incident angle used in the FDTD model is provided in the supporting information (Fig S10).

3. Results and discussion

The synthesis pathway for TiNT-dopamine-Ag triad nanocomposite is shown schematically in Fig. 1. In order to achieve control over the size and position of the silver nanoparticles $[Ag(NH_3)^2]^+$ was used as a source of silver, [22] resulting in a reduction on the terminal amine group of the dopamine molecules attached to the TiNT. As shown by TEM, Fig. 2, control over both size and position is achieved, with the nanotubes having a diameter of 8-9 nm and lengths of around 100 nm. The Ag nanoparticles have an average diameter of 8 nm; a size distribution histogram is shown in Fig. S1. As can be seen from Fig. 2c, the Ag nanoparticles exhibit a d-spacing of 0.14 nm, corresponding to the (220) lattice planes. [23] $AgNO_3$ was directly used as a source of silver but this resulted in the particle size being large and varied, with an average of 50 nm. In addition, there was no control over the position, as shown by TEM in Fig. S2. We also performed the synthesis at different Ag loading amounts: with too high a loading, the Ag particles aggregated together, and with too low a loading, large areas containing no Ag were seen in the TEM. This shown in Fig. S3 and S4.

The Ag content of the sample is 5 wt%, and the detailed experimental procedure is given in the experimental section. The TiNT-dopamine-Ag nanoparticle composites were characterized by UV-vis spectroscopy, shown in Fig. 3.

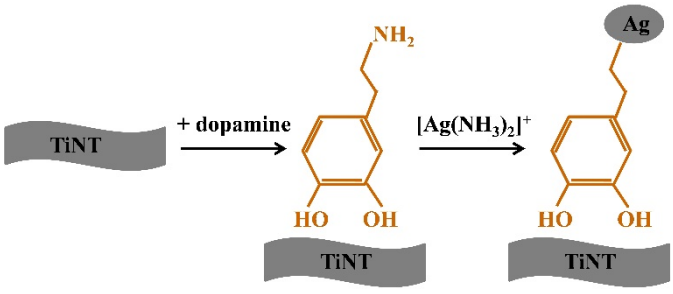

Fig. 1 Schematic reaction pathway.

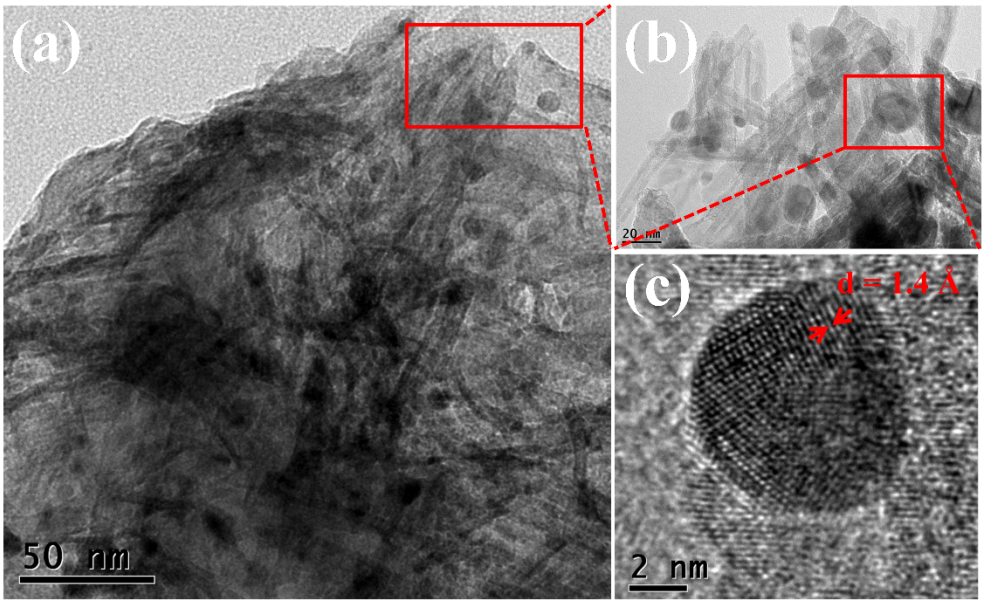

Fig. 2 TEM images of TiNT-dopamine-Ag composite.

In accordance with previously published results, the composite exhibits a shoulder upon dopamine functionalization, which is attributed to charge transfer, [14] and a band gap of 3.3 eV is calculated from the Tauc plot shown in Fig. S5. After reaction with $[Ag(NH_3)]^+$ to produce Ag nanoparticles both samples have an obvious increase in absorption in the visible range, which matches the now dark brown-black colour of the samples. Neither sample show a sharp LSPR peak and this will be discussed in a later section.

The XPS spectra of TiNT-dopamine-Ag was measured (Fig. 4); the survey spectrum is shown in Fig. 4a and the Ag 3d scan in Fig. 4 b. The Ag3d scan for TiNT-dopamine-Ag exhibits two peaks: at 374.3 eV, corresponding to the binding energy of Ag $3d_{5/2}$ and 368.3 eV, corresponding to Ag $3d_{3/2}$. These characteristic peaks with a spin-orbit separation of 6 eV are accounted for by the Ag^0 species. [16] The Ag XPS further supports the formation of Ag nanoparticles in the Ag^0 state.

Surface Enhanced Raman Spectroscopy

In our previous work, due to the bandgap of the composite being larger than the laser energy, it has been demonstrated that the TiNT-dopamine system is not activated for SERS by the lower energy 735 nm (1.687 eV) laser. [19] In this work, we use TiNT-dopamine-Ag excited with a higher energy, 532 nm (2.33 eV) laser to investigate the SERS enhancement. The results provide interesting insights into the cooperative effects of metal oxide organics and noble metal Raman enhancement.

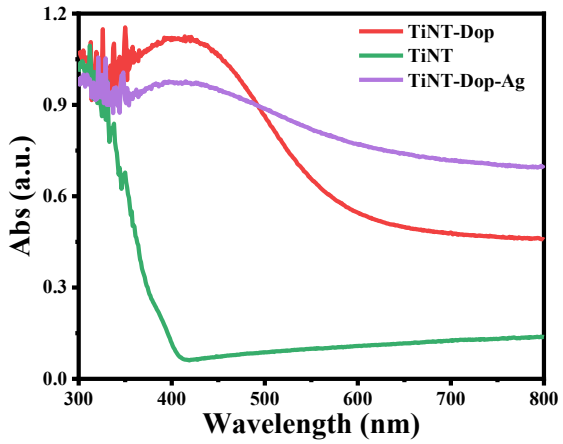

Fig. 3 UV-Vis spectra of the nanocomposites.

The Raman spectra of the composite is shown in Fig. 5a.The TiNT-dopamine-Ag sample has peaks assigned as Ti-O framework stretches at 160, 411 and 609 cm^{-1} and a peak that corresponds to covalent Ti-O-H bond at 768 cm^{-1}. Thin films of the nanocomposite material were prepared and the SERS activity was tested using methylene blue (MB) as a probe molecule. The MB solutions used had concentrations ranging from 0.03 to 30 nano molar. At higher MB concentrations, no linear dependence to intensity was seen. At lower concentration, no enhanced signal was clearly observed repeatedly.

Representative SERS spectra of various concentrations of MB on TiNT-dopamine-Ag are shown in Fig. 5b. (The corresponding intensity versus concentration of MB plots are shown in Fig. S6).

In addition, the enhancement factor (EF) for the SERS was calculated [17] according to the following equation:

$$EF = \frac{I_{sers}/N_{sers}}{I_R/N_R}$$

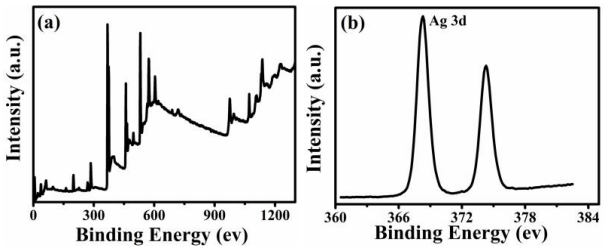

Fig. 4 XPS spectra of TiNT-dopamine-Ag (scan spectra, a and Ag 3d b).

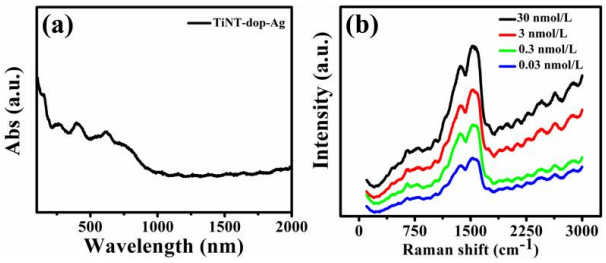

Fig. 5 Raman spectra of TiNT-dop-Ag (a) and representative Raman spectra of TiNT-dop-Ag with different concentrations of MB (b).

Where I_{SERS} and I_R are the intensities of the SERS and normal Raman signal at 1622 cm^{-1} and N_{SERS} and N_R are the number of MB molecules in the laser focus under SERS and normal conditions, respectively. The surface area of the laser spot was calculated to be 2.0588 x 10^{-11} m^2 and N_R was estimated to be 1.587 x 10^7. For the TiNT-dop-Ag system N_{SERS} was 1.435 x 10^3, giving an EF value of 3.816 x 10^6. Further details of the calculation are provided in the supporting information. As a comparison, we also prepared TiO_2-dopamine-Ag composites by a similar method and although a SERS effect was observed, it was of lower magnitude (details are provided in the supplementary information, Fig. S7-10). In both cases, the MB aliquot is allowed to dry on the surface, in a method analogous to a working sensor.

There are two components to SERS enhancement; Charge transfer and Electromagnetic Enhancement, therefore some insight was obtained by carrying out electromagnetic modelling. A thorough review of the Electromagnetic theories of SERS is given by Ding *et al*. [25] When the frequency of the Raman-scattered light is close to that of the incident light then the SERS enhancement factor due to the electric field at the position where the molecule is located (r_m) is given by:

$$EF(\omega_0, \boldsymbol{r}_m) \approx \left| \frac{\boldsymbol{E}(\omega_0, \boldsymbol{r}_m)}{\boldsymbol{E}_0(\omega_0, \boldsymbol{r}_m)} \right|^4 \qquad (1)$$

Where $\boldsymbol{E}(\omega_0, \boldsymbol{r}_m)$ is the electric field due to the incident field $\boldsymbol{E}_0(\omega_0, \boldsymbol{r}_m)$ at frequency ω_0 and position $\boldsymbol{r}_m$. Equation (1) is the well-known $|\boldsymbol{E}|^4$ approximation for the SERS enhancement factor.

It should be noted that charge transfer is normally considered to be caused by a chemical enhancement, as mentioned in the introduction. However, the enhanced electromagnetic field due to the LSPR of the Ag nanoparticle could also promote the charge transfer of hot electrons from the Ag to the TiNT. This process occurs when photoexcited electrons in the Ag can inject into the conduction band of a semiconductor and relax to the surface energy level.

Afterwards they can transfer to the lowest unoccupied molecular orbital (LUMO) of molecules that are absorbed on the semiconductor surface. [26-29]

Insight in to the SERS enhancement factor can be obtained by carrying out electromagnetic simulations of Ag particles on the surface of TiNT. The analysis was carried out using the Finite Difference Time Domain (FDTD) technique. [30] In the analysis the refractive index of TiNT was 1.8. Initially a TiNT was considered of 10 nm diameter with a Ag sphere, also of 10 nm diameter, on the surface. The electromagnetic model considered is depicted in Fig. S11.

A difficulty in the model was how to depict the properties of the dopamine, since data on the refractive index, and the thickness of the dopamine layers on the Ag and TiNT surfaces, was not available. A homogeneous dielectric material, of ε_r=3, filled the workspace rather than a vacuum or air. This was chosen to give plasmonic peaks close to the laser wavelength and, therefore, provide some possible indication of the magnitude of the electromagnetic enhancement factor possible.

Fig. 6 shows the result for absorption efficiency ($Q_{abs.}$) obtained from the FDTD calculation, where:

$$Q_{abs} = \frac{\textbf{scattering cross-section}}{\textbf{cross-sectional area of the Ag sphere}}$$

The calculation of $Q_{abs.}$ followed the procedure previously outlined in reference. [30] The inset in Fig. 6 shows the Electromagnetic enhancement factor for the TiNT case, at the absorption peak of 510 nm, for a cross section through the center of the Ag sphere from the model depicted in Fig. S10. As can be seen the electromagnetic enhancement is up to 6 orders of magnitude at the Ag-TiNT interface. It should be noted that large electric field enhancement may also lead to hot-electron transfer from the Ag to the semiconductor. Nevertheless, electromagnetic field enhancement is usually considered the dominant plasmonic process. [26]

However, we note with some caution that these calculations are only indicative of large electromagnetic enhancement being likely. Nevertheless, they do suggest that in the SERS measurements the Ag-TiNT case has a LSPR peak at, or very close to the laser wavelength. Although there is not a pronounced LSPR peak position for the TiNT-dop-Ag, the absorbtion spectra becomes wider band when the Ag is added.

It is our hypothesis that the laser wavelength used for the Raman experiments, 534 nm, matches the TiNT system. The size and position of Ag nanoparticles is well controlled through the fabrication process. This results in the large observed SERS enhancement. Importantly, we believe this efficient substrate design could lead to the future engineering of substrates for massive SERS enhancement through the accurate matching of the LSPR of metal nanoparticles to the SERS excitation wavelength.

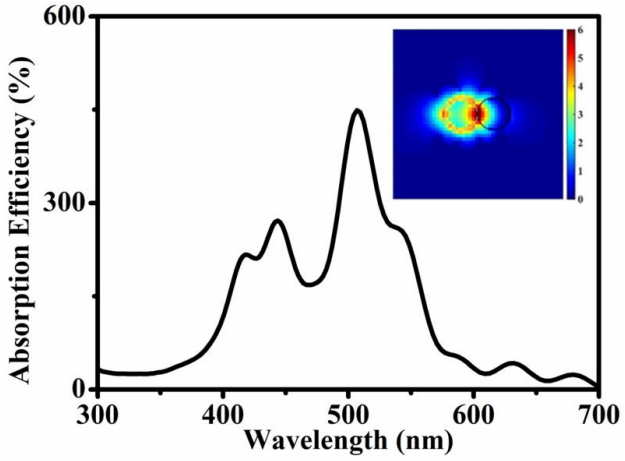

Fig. 6 Absorption efficiency for Ag-TiNT calculated using FDTD and inset electric field (E4) enhancement at 510 nm for Ag-TiNT. [Note: The scale is logarithmic]

The self-cleaning and photocatalytic properties of the composites were also tested and the results and experimental methods are shown in the supporting information, Fig. S12. If the composite were to be used as a recyclable sensor, the self-cleaning ability of the material is important. Our results show that the TiNT-dopamine-Ag composite has the ability

to degrade MB under UV illumination and be reused as a SERS detector. The photocatalytic properties of both TiNT-dopamine-Ag and TiO_2-dopamine-Ag were further investigated, shown in Fig. S13. Under these conditions all the MB is absorbed on the TiNT-dopamine-Ag system, and the TiO_2-dopamine-Ag system shows degradation activity.

To summarize, control over the size and position of the Ag nanoparticles in the TiNT-dop-Ag system along with LSPR matching the Raman excitation wavelength gives us an excellent SERS enhancement.

4. Conclusions

A composite of TiNT-dopamine-Ag nanoparticles was prepared and the SERS properties were tested experimentally, with supporting electromagnetic modelling. Control over the size and position of the Ag nanoparticles in the TiNT-dop-Ag system, along with matching of the LSPR of the Ag nanoparticle to the Raman excitation wavelength gives a SERS enhancement of 3.816×10^6. This efficient substrate design could lead to the future engineering of substrates for massive SERS enhancement through accurate matching of the LSPR of metal nanoparticles to the excitation wavelength.

5. References

1 J. R. Lombardi, R. L. Birke, *Acc. Chem. Res*., 2009, **42**, 734-742.
2 S. Schlucker, Surface Enhanced Raman Spectroscopy, Wiley, 2011.
3 M. Mulvihill, A. Tao, K. Benjauthrit, J. Arnold, P. Yang, *Angew. Chem. Int. Ed*., 2008, **47**, 6456-6460.
4 D. Graham, M. Moskovits, Z. W. Tian, *Chem. Soc. Rev*., 2017, **46**, 3864-3865.
5 K. Kasuga, M. Hiramatsu, A. Hoson, T. Sekino, K. Niihara, *Langmuir*, 1998, **14**, 3160-3163.
6 A. Thorne, A. Kruth, D. Tunstall, J. T. S. Irvine, W. Zhou, *J.Phys. Chem. B.*, 2005, **109**, 5439-5444.
7 Q. Chen, W. Zhou, G. Du, L.–M. Peng, *Adv. Mater.*, 2002, **14**, 1208-1211
8 S. Zhang, L.-M. Peng, Q. Chen, G. H Du, G. Dawson, W. Zhou, *Phys. Rev. Lett.,* 2003, **91**, 256103.;
9 D. V. Bavykin, J. M. Friedrich, F. C. Walsh, *Adv. Mater.,* 2006, **18**, 2807-2824.
10 I. Song, H. Lee, D. H. Kim, *ACS Appl. Mater. Interfaces*, 2018, **10**, 42249-42257.
11 X. Zhao, Y. Lei, G. Liu, L. Qian, X. Zhang, Y. Ping, H. Li, Q. Han, P. Fang, C. He, *RSC Adv*., 2020, **10**, 38715-38726.
12 J. Z. Wang, J. P. Zhou, Z. Q. Guo, y. x Lei, Q. U. Hassan, *Crys. Res. Tech.*, 2018, **53**, 1700153.
13 H. Li, J. Xi, A. G. Donaghue, J. Keum, Y. Zhao, K. An, E. R. McKenzie, F. Ran, *Sci Rep*, 2020, **10**, 10416
14 R. Liu, X. Fu, C. Wang, G. Dawson, *Chem. Eur. J*., 2016, **22**, 6071-6074.
15 Y. Xie, Y. Meng, *RSC Adv.*, 2014, **4**, 41734-41743.
16 S. C. Xu, Y. X. Zhang, Y. Y. Luo, S. Wang, H. L. Ding, J. M. Xu, G. H. Li, *Analyst*, 2013, **138**, 4519-4525.
17 Q. Y. Wang, J. S. Zhong, M. Zhang, D. Q. Chen, Z. G. Ji, *Mat. Lett.* 2016, **182**, 163-167.
18 Y. Chen, G. Tian, K. Pan, C. Tian, J. Zhou, W. Zhou, Z. Ren, H. Fu, *Dalton Trans.,* 2012, **41**, 1020-1026.
19 R. Liu, E. Morris, X. Cheng, E. Amigues, K. Lau, B. Kim, Y. Liu, Z. Ke, S. E. Ashbrook, M. Bühl, G. Dawson, *ChemistrySelect*, 2018, **3**, 8338-8343.
20 A. Centeno, F. Xie, N. Alford, *IET Nanobiotechnology*, 2013, **7**, 50-58.
21 A. F. Oskooi, D. Roundy, M. Ibanescu, P. Bermel, J. D. Joannopoulos, S. G. Johnson, A. Meep, *Computer Physics Communications*, 2010, **181**, 687-702.
22 Y. Cong, T. Xia, M. Zou, Z. Li, B. Peng, D. Guo, Z. Deng, *J. Mater. Chem. B*., 2014, **2**, 3450-3461.
23 A. Crake, K. C. Christoforidis, R. Godin, B. Moss, A. Kafizas, S. Zafeiratos, J. R. Durrant, C. Petit, *App. Cat. B: Envir*., 2019, **242**, 369–378.
24 D. V. Bavykin, J. M. Friedrich, A. A. Lapkin, F. C. Walsh, *Chem. Mat*., 2006, **18**, 1124- 1129.
25 S.-Y. Ding, E.-M. You, Z.-Q. Tian, M. Moskovits, *Chem. Soc. Rev.,* 2017*,* **46**, 4042-4076.
26 L. Yang, Q. Sang, J. Du, M. Yang, X. Li, Y. Shen, X. Han, X. Jiang, B. Zhao, *Phys. Chem. Chem. Phys.,* 2018*,* **20**, 15149-15157.;
27 G. V. Hartland, L.V. Besteiro, P, Johns, A. O. Govorov, *ACS Energy Lett.,*2017*,* **2**, 1641-1653.
28 C. Clavero, *Nat. Photonics* 2014*,* **8**, 95-103.
29 X. Cheng, S. Gu, A. Centeno, G. Dawson, *Scientific Reports*, 2019, **9**, 5140.
30 A. Centeno, A. Bader, H. Reehal, F. Xie, *Nanotechnology*, 2013, **24**, 415402.